NRC Publications Archive
Archives des publications du CNRC

A practicable formulation for the strength of glass and its special application to large plates
Brown, William C.

For the publisher's version, please access the DOI link below./ Pour consulter la version de l'éditeur, utilisez le lien DOI ci-dessous.

https://doi.org/10.4224/23002290

National Research Council Canada   Conseil national de recherches Canada

Canada

A PRACTICABLE FORMULATION FOR THE STRENGTH
OF GLASS AND ITS SPECIAL APPLICATION TO
LARGE PLATES

by

W. G. Brown

National Research Council of Canada, Ottawa

*A PRACTICABLE FORMULATION FOR THE
STRENGTH OF GLASS AND ITS SPECIAL
APPLICATION TO LARGE PLATES

by

W.G. Brown

(2nd draft, August 1970)

SUMMARY

A simplified description of delayed failure including time, temperature and relative humidity effects was incorporated into appropriate mathematical statistics to yield a generalized failure probability relationship for glass. Practicability was demonstrated by correlating test results for large areas of soda-lime plate glass from independent manufacture sources. (The test results demonstrate a range of load-bearing capacity of about 2:1 as a result of loading duration differences of 30:1 and surface area differences of 9:1). To supplement the description of delayed failure, two additional statistical parameters describing the strength of this kind of glass were established with the help of a separate stress-distribution investigation. Several examples were worked to show application in glass design.

CONTENTS

INTRODUCTION

Almost 50 years have passed since Griffith (1) brought
attention to the weakening effect of pre-existing surface flaws
or scratches in glass. As a result of the stress raising effect
of these flaws, the measured failure strength of glass in tension
is usually several orders of magnitude lower than its theoretical
strength. That this effect is real is borne out by the results
of many tests since Griffith's time which show that average
measured strengths and frequency distributions are altered by
deliberate surface conditioning; for example, sand blasting,
grinding, polishing, or etching. Surface roughening results
in reduced average strength and reduced variability, whereas
smoothing operations result in increased strength with attendant
increased variability. It has been aptly pointed out that the
observed strength is not a property of the glass materials; it
is, rather, a derived function of both glass properties and flaw
geometry.

Measured strength, however, is not solely dependent on
surface treatment; the average measured failure stress in moist
air at room temperature is noted to decrease with increased
duration of loading. This important phenomenon of delayed
failure as dependent on atmospheric moisture content and tem-
perature has been investigated in considerable detail,

particularly during the past decade. It is now generally accepted that slow flaw growth takes place as a result of stress corrosion combined with plastic-viscous flow.

The present work had modest beginnings in that it was intended to improve upon the empiricism of window design. It became apparent, however, that while extensive engineering tests had recently become available, they had been carried out without reference to contemporaneous scientific investigations on the effect of loading duration. Furthermore, neither the engineering tests nor the load duration results offer a description of the strength of glass; they only yield measurements of the strength of different glass objects under specific loading conditions. That the strength of glass has not been described, however, is only due to the fact that load duration effects have not been generalized and combined with probability theory. A complicating factor is that of stress variations over the glass surfaces.

The intent of the present work is to develop and demonstrate a practicable formulation for the strength of glass. By this is meant a straightforward mathematical scheme that describes glass strength as a failure probability relationship incorporating the most important aspects of delayed failure. While the mathematical generalization of delayed failure can be confirmed by tests from several independent sources, it is

the engineering tests which permit demonstration of the
practicability of the complete formulation, for it is only in
these tests that both loading rate and glass size were varied.
Nevertheless, the open literature has revealed only two
independent sets of tests that have been carried out in
sufficient detail for this purpose. (A third, limited set
of tests is also available.) The very high cost of these tests
($\approx$ \$5 x 10^5) justifies deriving as much value as possible from
them. The test results will be shown to correlate on the basis
of the complete glass strength formulation, and to yield two
statistical parameters which describe the strength of large
elements of commercial, soda-lime plate glass. Several examples
are worked to show applicability in design.

Although the present analysis has been limited by
circumstances to consideration of plates of a specific glass
material, the general formulation should be equally applicable
to objects of any particular glass material with any particular
kind of surface treatment.

THEORETICAL

Delayed failure of glass in the presence of water vapour

For present purposes, it is not necessary to review again many important earlier investigations on glass behaviour. An excellent resume is given by Wiederhorn (2). In order to discuss and generalize the implications of experimental results on delayed failure, however, it is first necessary to have available a simple conceptual model for the process. Much of this is already available in the work of Charles (3,4) and Charles and Hillig (5,6).

Since water vapour induces chemical corrosion in glass Charles (3,4) supposes a simple rate equation of the form,

$$\frac{dz}{dt} = Ke^{-\gamma/RT} \tag{1}$$

Where: $\frac{dz}{dt}$ is the rate of progress of the glass interface perpendicular to its surface,

K is a pre-exponential constant,

R is the gas constant,

T is absolute temperature,

γ is an activation energy.

By direct measurement of the rate of corrosion
penetration in unstressed soda-lime glass (Corning 0800)
Charles obtains an activation energy γ of 20 ± 4 K cals/mol for
the initial stage of corrosion.

In applying equation (1) to corrosion in pre-existing
cracks in glass, Charles and Hillig (5,6) assume the activation
energy γ to be, additionally, stress-dependent and, as well, to
depend on the free energy of the corrosion reaction and possible
plastic or viscous deformation. These additional terms, of
somewhat speculative nature and magnitude, are considered to be
of importance only at low stresses where they result in a
fatigue limit stress below which failure will not occur.
Available test results, however, have been carried out in
stress ranges where no limit is apparent; consequently, for
present purposes γ will be considered to be dependent on
stress alone.

Marsh (7), on the other hand, considers plastic-
viscous flow to be of major importance in the delayed failure
process. While it is not possible to reconcile this concept
in mathematical detail with Charles' and Hillig's subsequent
derivations, it can be shown, nevertheless, that identical
generalizations result.

Making use of a mathematical solution for the stress distribution about a two-dimensional elliptical crack, Charles and Hillig derive from equation (1) an expression for the rate of change of geometry of a pre-existing flaw. With:

$$\gamma = \gamma_o - \gamma_1(\sigma) \tag{2}$$

their equation (7) reduces to:

$$\frac{d(\frac{x}{\rho})}{dt} = \frac{K_1}{x} \left(\frac{x}{\rho}\right)^2 \cdot e^{-\gamma_o/RT} \cdot \frac{\gamma_1(\sigma)}{RT} \cdot e^{\gamma_1(\sigma_m)/RT} \tag{3}$$

for large x/ρ. Here x and ρ are the depth and tip curvature radius, respectively, of the flaw; K_1 is a constant; and σ_m is the tensile stress at the flaw tip. The form of $\gamma_1(\sigma)$ is unknown a priori, but

$$\sigma_m \approx 2\sigma \left(\frac{x}{\rho}\right)^{1/2} * \tag{4}$$

where σ is the applied stress at the glass surface.

There are several possibilities for imperfection in equation (3). Firstly, no allowance was made for changing stress distribution as the flaw geometry changes. Secondly, the flaw width at its tip may be, or may reach the limiting spacing of the glass molecules. Thirdly, equation (4) may not apply well for the very small dimensions and high stresses at a flaw tip.

---

* This is the Inglis stress concentration relationship (8) for large x/ρ.

In his earlier papers Charles (3,4) had assumed empirically that

$$\frac{d(\frac{x}{\rho})}{dt} = K_2 \cdot \sigma_m^{\ n} \cdot e^{-\gamma_0/RT} \quad . \tag{5}$$

The resulting integrated form was found to correlate experiment with good precision. Almost the same result is obtained by treating x/ρ and t as piece-wise separable in equation (3), thus:

$$\frac{x}{K_3} \cdot \frac{d(\frac{x}{\rho})}{(\frac{x}{\rho})^{2+n/2}} = (\frac{\sigma}{T^\alpha})^n \cdot e^{-\gamma_0/RT} \cdot dt \tag{6}$$

where n and α are constants.

Experimentally, n turns out to be large and constant to high degree, thus, as pointed out by Charles, the value of $(x/\rho)^{2+n/2}$ at or near failure is much greater than the initial value. It follows that for a specific flaw which leads to failure,

$$\int_o^{t_f} (\frac{\sigma}{T^\alpha})^n e^{-\gamma_0/RT} \ dt \approx constant \tag{7}$$

Here t_f is time to failure.

In order to accommodate Marsh's plastic-viscous flow into equation (6) it is only necessary to assert that the

exponent on $(\frac{x}{\rho})$ remains large. It is then immaterial whether flaw geometry changes occur as a result of changes in x or ρ or both, and equation (7) applies as before.

Experimental verification

Although implied, Charles did not complete the generalization of equation (7). Rather, he carried out the integration for the two cases of σ constant, and σ increasing at constant rate. Charles' experimental results for bending of small rods of soda-lime glass (Corning 0800) in saturated water vapour are given in Figures 1 to 3. In Figure 1 (constant σ), it is only at temperatures below about -50°C that noticeable deviation from the constant n form of equation (7) becomes apparent. This deviation is a result of the presumably approximate nature of equation (6) and neglect of the secondary term for $\frac{x}{\rho}$ in integration of equation (6). Figure 2 gives measured average failure stresses at 25°C for constant rate of load application. Figure 3 gives Charles' determination of γ_o = 18.8 K cal/mol as obtained by setting α = o in equation (7). In developing equation (2), however, Charles and Hillig expanded γ as

$$\gamma = \gamma_o + \frac{d\gamma}{d\sigma}\bigg]_o \sigma + \ldots\ldots \tag{8}$$

This form indicates $\alpha = 1$ as a first approximation. As may be seen from Figure 3, this assumption yields $\gamma_o = 25$ K cal/mol and gives a correlation which is considerably improved in the high temperature range. (Since the upper and lower limits of Figure 3 have been obtained by extrapolation, there appears to be no merit in attempting to obtain a more precise value for α.)

Wiederhorn (2,9) has observed the rate of progress of large, artificial cracks. For relative humidities greater than about 5% at room temperature and velocities $(\frac{dx}{dt})$ less than about 0.01 mm/sec, his results are consistent with the forms of equations (1) and (6) but not sufficiently detailed to distinguish between them. At higher velocities Wiederhorn's observations indicate an effect attributable to the limitations of diffusion of water vapour to the crack tip. At still higher velocities, crack progress becomes independent of relative humidity. Obviously, however, high velocities will only be operative for very short times in glass failure; consequently, low velocity growth will ordinarily predominate overwhelmingly in equation (7).

Wiederhorn (9) also investigated the effect of relative humidity on crack velocity. His theoretical development indicates velocity to be approximately proportional to relative humidity

raised to the power of the number of water molecules reacting with a single glass bond. Experimentally, this number appears to be 1 for relative humidity greater than 1 to 10%; for lower values of RH the number appears to be 1/2. Charles (3) carried out one series of tests at 50% RH which yielded strengths about 7% higher than at saturation. This appears to be consistent with Wiederhorn's work indicating velocity directly proportional to RH (this would indicate strength at 50% RH to be 4.6% higher than at saturation).

Mould and Southwick (10) investigated delayed failure in constant load bending of wet, artificially roughened microscope slides with various abrasions. Close inspection of their results shows that while the individual series of tests show some irregularity there is no recognizable deviation from the form of equation (7) with n = 16 as found by Charles.

Some constant rate of loading results (constant temperature, 296°K) by Kropschott and Mikesell (11) are given in Table I and compared with prediction by equation (7)

Table I

Loading rate β	Comparative average failure stress	Predicted $(\beta^{1/17})$
1 psi/sec	1.00	1.00
10 psi/sec	1.11	1.14
800 psi/sec	1.48	1.49

On the basis of apparent general agreement with experimental data, equation (7) appears to be adequate to describe the delayed failure characteristics of glass in water vapour. Introducing Wiederhorn's relative humidity effect for soda-lime glass, in particular, the result is, again, for any specific flaw which leads to failure:

$$\int_o^{t_f} RH \ e^{-\gamma_0/RT} \ (\frac{\sigma}{T})^n \ dt \approx constant = S \qquad (9)$$

Here, RH is the decimal relative humidity. For the special situation, in particular, of $\sigma = \beta_o t$, (β_o constant), for one-dimensional tensile stresses at constant temperature T_o and constant relative humidity RH_o, equation (9) becomes :

$$\sigma_\varepsilon = C\{\int_o^t RH \cdot e^{-\gamma_0/RT} \cdot (\frac{\sigma}{T})^n \ dt\}^{\frac{1}{n+1}} \qquad (10)$$

where:
$$C = \{\frac{\beta_o \ T_o^n \ (n + 1)}{RH_o \ e^{-\gamma_0/RT_o}}\}^{\frac{1}{n+1}} \qquad (11)$$

and σ_ε is the failure stress for the condition $\sigma = \beta_o t$.

From equation (10), it may be seen that for samples arbitrarily stressed in tension at temperature T and relative humidity RH (all time-dependent) for time t there corresponds a specific stress σ_ε and, consequently, a specific failure probability P.

While it is clear that stress alone is not a failure criterion, nevertheless, equation (10) makes it possible to retain this simple concept in the sense of a stress-equivalent. This concept will be used in most of the remaining portion of this paper.

Appropriate mathematical statistics for glass

As indicated in the introduction, the initial flaw size distribution in a set of samples will generally be arbitrary, i.e. not conforming to any of the well known mathematical distribution functions. Under the circumstances, it is thus entirely permissible to choose a continuous function which offers the simplest approximate mathematical description of test results. This is the Weibull function.

In his important paper, Weibull (12) proposes a relationship between failure probability and stress of the form:

$$P_{Ao} = 1 - e^{-k\sigma\epsilon^{m}} \tag{12}$$

for samples of a given surface area, A_o. Here k and m are experimental constants.

In actual fact, surface stresses will always be two-dimensional. As shown in Appendix I, however, there exists a one-dimensional stress-equivalent at every surface location. Consequently, accepting only that glass failure is a weakest-link, surface* phenomenon, the probability of failure of area

*A strength-volume effect of negligible magnitude is probably also present. In addition, the cut edges of glass, if in tension, experience a severe strength-line effect.

elements of size $A = NA_o$, can be written:

$$P_A = 1 - \exp[-k(\frac{A}{A_o}) \, \Sigma_1^N \, \sigma_\varepsilon^m]^\dagger \qquad (13)$$

Application to rectangular plates

For the special case of rectangular plates, σ_ε can be written:

$$\sigma_\varepsilon = \sigma_{\varepsilon c} \cdot f(\frac{x}{a}, \frac{y}{\ell}, t) \qquad (14)$$

whence, equation (13) becomes :

$$P_A = 1 - \exp[-k(\frac{A}{A_o}) \cdot I \cdot \sigma_{\varepsilon c}^m] \qquad (15)$$

where

$$I = \int_0^1 \int_0^1 [f(\frac{x}{a}, \frac{y}{\ell}, t)]^m \, d(\frac{x}{a}) \cdot d(\frac{y}{\ell}) \qquad (16)$$

Here, x and y are coordinates on a plate of width a and length ℓ, and $f(\frac{x}{a}, \frac{y}{\ell}, t)$ symbolizes σ_ε varying with position and time. $\sigma_{\varepsilon c}$ is a convenient reference value for the one-dimensional stress equivalent, usually that at the plate center.

Approximation:

Some mathematical difficulty now arises in computing I as a result of the fact that the relative stress distribution in plates ordinarily changes with changing pressure load.* To avoid

---

†The equivalent expression for a glass edge, obtainable with the help of equations (10,11,12) is:

$$P_\ell = 1 - \exp[-kC^m(\frac{\ell}{\ell_o}) \int_0^1 \{(\frac{\sigma}{T})^n \, RH \cdot e^{-\gamma_0/RT} \, dt\}^{\frac{m}{n+1}} \, d(\frac{x}{\ell})]$$

Here, σ is the tensile stress on the edge of length ℓ, and ℓ_o is a reference length. In general, k and m will differ from glass surface values.

*The deflections of thin glass plates usually fall in the non-linear range where both bending and membrane stresses are important.

obviously unwarranted amounts of computation, however, it is shown in Appendix II that, as an approximation, the product $I \cdot \sigma_{\epsilon c}{}^m$ in equation (15) can be replaced by

$$\eta = C^{\dot{m}} \left[\int_0^t (rI)^{\frac{n+1}{m}} \cdot \left(\frac{\sigma_{uc}}{T}\right)^{\dot{n}} \cdot RH \cdot e^{-\gamma_0/RT} \, dt \right]^{\frac{m}{n+1}} \qquad (17)$$

(The detailed definitions of r and I for equation (17) are given in Appendix II.)

Stress distribution:

For thin, uniformly loaded, rectangular glass plates with edges free to move in their plane, elastic theory requires a relationship between stress σ and pressure load q of the general, non-dimensional form:

$$\frac{\sigma}{E} \left(\frac{a}{h}\right)^2 = Q\left[\frac{q}{E} \left(\frac{a}{h}\right)^4 , \frac{Eh^3}{a}\xi , \frac{\ell}{a}\right] \qquad (18)$$

where: σ is any specific stress at surface location $\left(\frac{x}{a} , \frac{y}{\ell}\right)$

E is Young's modulus

h is plate thickness

ξ is an edge restraint constant, defined as $\xi = \frac{1}{M_o} \frac{dW}{dx}]_o$. ($M_o$ is the edge bending moment and $\frac{dW}{dx}]_o$ is the slope of the deflection surface at the edge. For present purposes ξ is assumed constant along all edges.)

for constant $\frac{Eh^3}{a}\xi$ and $\frac{\ell}{a}$, both $\frac{\sigma}{E}\left(\frac{a}{h}\right)^2$ and the product rI depend

only on $\frac{q}{E}(\frac{a}{h})^4$. Thus, for a limited range of $\frac{q}{E}(\frac{a}{h})^4$, it is permissible to write:

$$rI^{\frac{n+1}{m}} \cdot \sigma_{uc}^n = E^n (\frac{h}{a})^{2n} \cdot B[\frac{q}{E}(\frac{a}{h})^4]^s \tag{19}$$

$$= B \cdot E^{n-s} \cdot (\frac{a}{h})^{4s-2n} \cdot q^s \tag{20}$$

Where B and s are constants for a particular range of $\frac{q}{E}(\frac{a}{h})^4$. Inserting equation (20) into equation (17), and equation (17) into equation (15) now gives:

$$P_A = 1 - \exp[-kC^m \frac{A}{A_o} \{B \cdot E^{n-s} \cdot (\frac{a}{h})^{4s-2n} \int_o^t \frac{RH}{T^n} \cdot e^{-\gamma_o/RT} \cdot q^s dt\}^{\frac{m}{n+1}}] \tag{21}$$

This is a practicable, generalized failure probability relationship for uniformly loaded rectangular plates, incorporating effects due to plate geometry, area, load duration, relative humidity and temperature. The constants B and s obtain from elastic theory or elastic tests, while k and m must be determined from failure tests.

CORRELATION OF TESTS ON PLATES

Available experimental data

Only the following results (for commercial soda-lime glass) have been reported in such a way that they are amenable to analysis:

(1) Bowles and Sugarman (13) carried out detailed tests on 210 panels of 41" x 41" plate and sheet glass manufactured by Pilkington Bros. (U.K.) with thickness varying between 0.11 inches and 3/8 inches. The glass was uniformly loaded and edges were supported without restraint (simple support). The tests were carried out at approximately constant rate of change of deflection to cause breakage in about 30 seconds. The results are summarized in Table II.

(2) A very extensive series of proprietary tests on over 2000 lights of plate and sheet glass of various thicknesses up to 3/4" and sizes up to 10 feet by 20 feet has been carried out by the Libbey-Owens-Ford Glass Co. (U.S.A.) (14). The test results have only been made public in the form of charts (Figure 4) which, however, can be compared with the Bowles and Sugarman work. These tests were also carried

out at approximately constant rate of change of deflection:
actually center deflection was increased in increments of
0.1 inches and held for 60 to 75 seconds at each value (60
seconds nominal plus up to 15 seconds for adjustment.
Since deflection at failure was about 1 inch for the
larger plates, the total loading time was about 35 times
greater than in the Bowles and Sugarman tests.

(3) More limited tests similar to the above on fewer, (20)
lights, (Pittsburgh Plate Glass Co., U.S.A.) are reported
in somewhat more detail by Orr (15). Although very
limited in number, the results do not appear to differ
greatly from those of Figure. 4. The principal value of
Orr's work here, however, is that it indicates the effect
that edge glazing may have on deflection and stresses.

Deflections in simply-supported square plates

In order to make use of equation (21) in comparing
the Bowles-Sugarman and L-O-F data, it is necessary to specify
the variation of q with time. In both cases the plates were
loaded such that the centre deflection was increased approxi-
mately linearly with time. Since Bowles and Sugarman deter-
mined the relationship between load and deflection, it is thus
possible to establish the time variation of q.

Elastic theory (e.g. (16)(17)) requires a relation-ship between load and deflection of the form:

$$q = \frac{20.6E}{(1-v^2)} \left(\frac{h}{a}\right)^4 \left(\frac{W_o}{h}\right)[1+C_1(1-v^2)\left(\frac{W_o}{h}\right)^2 +C_2(1-v^2)^2\left(\frac{W_o}{h}\right)^4 +\ldots] \quad (22)$$

where W_o is the plate centre deflection and v is Poisson's ratio ($\simeq 0.22$ for glass).

In Figure 5, $\frac{W_o}{h}$ has been plotted against $\frac{q}{E}\left(\frac{a}{h}\right)^4$ for the data of Table II, with E assumed to be 1.0×10^7 psi. Also included in the figure are the deflection measurements of Kaiser (18) which were carried out on a steel plate ($v = 0.33$). (In plotting, Kaiser's results have been converted to equivalent glass results by taking due account of the different v values (17).) Kaiser's experimental and theoretical values for C_1 were apparently identical ($C_1 = 0.176$). For the Bowles-Sugarman results, however, a considerably larger range of variables was covered and retention of C_2 in equation (22) improved correlation at high values of W_o/h. The curve for W_o/h in Figure 5 is, (for glass):

$$q\left(\frac{a}{h}\right)^4 = 2.15 \times 10^8 \left(\frac{W_o}{h}\right)(1+0.165\left(\frac{W_o}{h}\right)^2 -0.0007\left(\frac{W_o}{h}\right)^4) \quad (23)$$

That the works of Kaiser and of Bowles and Sugarman agree so well is an indication that both studies were carried out with true simple support.

Evaluation of experimental results

Both the L-O-F and Bowles-Sugarman tests were such that:

$$q = C_3 t^{1/b} ; \qquad (24)$$

to a close approximation. Here C_3 and b are constants which differ in each test series. From equation (24);

$$dt = \frac{bq^{b-1}}{C_3^b} dq . \qquad (25)$$

Substituting (25) into (21) and performing the integration gives, (assuming T, RH, constant):

$$P_A = 1-\exp[-kC^m \cdot \frac{A}{A_o} \{\frac{RH}{T^n} e^{-\gamma_0/RT} \cdot B \ E^{n-s} \cdot (\frac{a}{h})^{4s-2n} \frac{b\bar{t}}{(s+b)} \cdot \frac{q^{s+b}}{\bar{q}^b}\}^{\frac{m}{n+1}}] \qquad (26)$$

Here, $\bar{t}$ is the average time to failure corresponding to $\bar{q}$, (equation (24)).

The average pressure at failure, $\bar{q}$ corresponds to a specific, constant failure probability for all test series, thus re-arranging equation (26) for $q = \bar{q}$ there results:

$$\bar{q} \cdot (\frac{a}{h})^{4-2n/s} \cdot (\frac{b\bar{t}}{(s+b)})^{\frac{1}{s}} \cdot \frac{A}{A_o}^{\frac{n+1}{ms}} = \text{constant} \qquad (27)$$

The exponent b is obtained by differentiation of equation (23), i.e.:

$$b = \frac{1+0.165(\frac{\bar{W}_o}{h})^2 -0.0007(\frac{\bar{W}_o}{h})^4}{1+3\times0.165(\frac{\bar{W}_o}{h})^2 -5\times0.0007(\frac{\bar{W}_o}{h})^4} \qquad (28)$$

None of the experimental studies reported temperature
or relative humidity -- it is, therefore, necessary to assume
room temperature (21°C) and average relative humidity (50%) in
all cases.

The light edge restraint in the L-O-F tests consisting
of 1/8" x 3/8" neoprene gasketting in 1/8" x 3/4" aluminum
angles was roughly similar to that used by Orr (15), where
analysis shows it to have a considerable effect on the deflec-
tions of plates thinner than about 3/8" with shortest side
about 6 ft. As a result, consideration should be limited
approximately to these dimensions in Figure 4, to ensure
nearly simple support for comparison with the Bowles and
Sugarman work. For square plates, however, there are two
factors that permit larger square plates to be considered.
These are: (1) the glazing has a smaller relative effect on
stresses in square plates than in rectangular plates; and
(2) the larger plates of given thickness deflect so far into
the large deflection range that membrane stresses (almost
independent of edge restraint) form a large portion of the

combined membrane-bending stresses. This is indicated by the four reported tests by Orr on 82" x 82" square plates which have been included with the Bowles-Sugarman data in Figure 5. (Plate thicknesses 0.237", 0.240", 0.303", 0.301".)

Table III lists the pertinent sizes of square plates for each of which 25 samples were tested by L-O-F. To determine $\bar{W}_o$, the values of $\bar{q}$ were taken off Figure 4 and inserted into equation (23). The average times to failure were then determined from the loading rate (i.e. about 75 seconds per 0.1 inch of deflection). Values of b were then determined from equation (28). Equation (28) was also used to determine the values of b for the Bowles and Sugarman data of Table II.

Correlation procedure

First attention will be given to the Bowles and Sugarman data since these are more thoroughly specified than those of L-O-F. In equation (27) preliminary consideration shows that s is a large number. Thus, the exponent on $b\bar{t}$ is small and since $b\bar{t}$ (Table II) does not differ greatly for all tests, a first estimate of s is obtained by plotting $\bar{q}$ vs h, Figure 6. Bowles and Sugarman calculated the 95% confidence range on $\bar{q}$, the limits of which are also shown with the data.

The results for sheet and plate glass differ appreciably in Figure 6; apart from the fact that sheet glass appears to be about 25% stronger than plate glass, however, discussion will henceforth be confined to the plate glass results since no other sheet glass data is available for comparison. Accepting the apparent slope of 1.4 for the plate glass in Figure 6, there results from equation (27): $4 - 2n/s = 1.4$, whence, with $n = 16$, $s = 12.3$.

Parameter m and coefficient of variation

The fact that Bowles and Sugarman recorded the coefficient of variation (ν) on q and on W now permits an estimate of parameter m for their data. Weibull (page 13) gives an equation and table, Appendix III, relating the exponent $(n+1)/m(s+b)$ in equation (26) to the coefficient of variation on q. Although there can be little precision on determination of this coefficient for only 30 or 40 samples in each set, nevertheless, the apparent increase in ν_q with increasing thickness in Table II appears to be the result of minor experimental error arising from over-lapping pressure measurements on different gauges. This becomes apparent when the coefficient on q is determined from that on W. Assuming negligible variation in h (as reported by Bowles and Sugarman) this requires $\nu_q = \nu_w/b$. The values of ν_q calculated in this

way are also given in Table II, where they show considerably increased uniformity for plate glass but are inconclusive for the more limited sheet glass results. Accepting a mean value of ν_q = 21.5% for all plate glass results, Table VI (Appendix III) gives $\frac{m(s+b)}{n+1} = 5.5$,

whence, m = 7.3.

The exponent on A/A_o in equation (27) thus becomes $\frac{n+1}{ms} = \frac{1}{5.3}$.

In Figure 7 values of $\bar{q}(\frac{A}{A_o})^{\frac{1}{5.3}}(\frac{b\bar{t}}{12.3+b})^{\frac{1}{12.3}}$ have been plotted against $(\frac{h}{a})$ for both the L-O-F and Bowles-Sugarman data. (The reference area A_o has been taken to be 1.0 sq ft.) Agreement between the two sets of data is exceptional.

Implications of the correlation

The simplest way to illustrate the direct implications of Figure 7 is to compare the actual breaking pressures $\bar{q}$ of Table III (L-O-F) with those that would be obtained by designing from the Bowles and Sugarman data with the unreliable ad hoc assumption that failure occurs independently of load duration and plate area when the stresses are the same in both cases. For this purpose, equation (18) shows it is only necessary to enter Figure 6 with an equivalent thickness h_ε = h(40.5/a), (where h and a are the actual thickness and plate width in inches in the L-O-F tests). The results are summarized in

Table IV where column (3) gives the indicated breaking pressure and column (4) gives the ratio of indicated to actual breaking pressures. The ratio has the significantly large range of 1.4 to 1.9 depending on the plate size. This means that the smaller, more rapidly loaded plates of the Bowles-Sugarman tests will withstand loads 40% to 90% greater than the larger, slowly loaded plates of the L-O-F tests. Column (5) shows that approximately 1/3 of the load increase is attributable to load duration differences, while the remainder (between about 1/4 and 1/2, column (6)) is due to area differences. Column (7) gives the combined calculated effect of load duration and area. The values are sufficiently close to those of column (4) that further attempts at refinement do not appear warranted at this time.

It appears likely that most of the residual difference of about 15% between the two sets of data in Figure 7 is attributable to the edge glazing in the L-O-F tests. This being so, then Figure 7 may fairly represent universal strength characteristics for ordinary soda-lime plate glass. As pointed out previously, the limited tests by Orr (15) using plate glass from a third (PPG) source indicate essential agreement with the L-O-F results. It seems then that there is sufficient evidence supporting the universality of Figure 7 to pursue the problem

further to obtain, in addition to m, a value of k (equation
(12)):   thereby, the strength characteristics of this type of
glass will be completely determined for the structural usage
range.   Determination of k is made possible by the investiga-
tion of Kaiser (18) who measured the two-dimensional stress
distribution over the surface of a thin, square plate.   With
k determined, any plate glass structure may subsequently be
designed after determining surface stress distribution either
by strain measurements or from elastic theory.   No further
failure tests are necessary.

Should it turn out, on subsequent investigation,
that Figure 7 is not representative of all plate glass, then
the values of k and m here established apply, in any event,
specifically to the commercial glass tested by Bowles and
Sugarman.

The procedure for determining parameter k is given
in Appendix IV, and all parameters are summarized below:

Strength characteristics of large
areas of soda-lime plate glass

Based on one-dimensional tensile tests on specimens
of one square foot area, at a rate of stress increase
of β_o = 100 psi/second at 295°K and 50% relative
humidity:

$$m = 7.3$$
$$k = 5 \times 10^{-30} \text{ psi}^{-7.3}$$
This paper

$$\gamma_o/R = 12,600°K$$
$$m = 16$$
Charles (3)

Insertion of these values into equation (21) gives
the probability of failure of a plate as dependent on the
strength parameters, the plate geometry and the manner and
duration of uniform pressure loading. In design, interest
centers on maintaining a low value for failure probability.
In this case, equation (21) simplifies to, after inserting all
parameters;

$$P_A \simeq 1.23 \times 10^{-28} A [B \ E^{16-s} (\frac{a}{h})^{4s-32} \int_0^t (\frac{RH}{0.5}) (\frac{T_o}{T})^{16} \ e^{-\frac{\gamma_o}{R}(\frac{1}{T}-\frac{1}{T_o})} q^s dt]^{0.43}$$

(29)

Equation (29) can also be re-arranged to permit an estimate of
the required glass thickness to withstand a given load with a
given failure probability, i.e.;

$$\frac{h}{a} = \left[\left(\frac{1.23 \times 10^{-28} A}{P_A}\right)^{\frac{1}{0.43}} B \ E^{16-s} \int_o^t \left(\frac{RH}{0.5}\right)\left(\frac{T_o}{T}\right)^{16} e^{-\frac{\gamma_o}{R}\left(\frac{1}{T}-\frac{1}{T_o}\right)} q^s dt\right]^{\frac{1}{4s-32}}$$

$$(30)$$

Here the thickness h and plate width a are in consistent units, A is the plate area in sq ft, q and E are in psi, and time t is in seconds. T_o is the absolute reference temperature, assumed to have been 295°K in the reported tests. B and s are general parameters dependent on edge restraint and plate shape.

Examples

Ideally, all design should be based on a pre-established probability of failure during the lifetime of a structure. In this section, a simple comparison will be made of the thickness of glass plates with different edge support which have the same failure probability under a given, arbitrary, uniform pressure loading of specified duration.

Other than the work of Kaiser for simply supported square plates, the literature does not immediately appear to contain stress distribution solutions, that are pertinent to the types of edge support encountered with real plates. At present, then, examples are necessarily limited to somewhat arbitrary conditions. A simple solution is available, however, for rectangular plates supported on two opposite sides. Since this solution approaches that of long narrow plates supported

- 28 -

on all sides, it will be useful for illustrative purposes to
compare its thickness requirements with those for simply
supported square plates.

For rectangular plates identically supported only on
two opposite sides, the surface stress distribution is as
follows:

$$\frac{\sigma_x}{E}\left(\frac{a}{h}\right)^2 / \frac{q}{E}\left(\frac{a}{h}\right)^4 = 3\left[\left(\frac{x}{a}\right)-\left(\frac{x}{a}\right)^2 - \frac{1}{6\left(1+2\frac{D\xi}{a}\right)}\right] , \tag{31}$$

$$\sigma_y = \nu\sigma_x , \tag{32}$$

where $D = \frac{Eh^3}{12(1-v^2)}$, is the modulus of rigidity; $\tag{33}$

$\xi = 0$ represents fixed support and $\xi = \infty$ represents simple
support.

The relative tensile stresses of equation (31)
occurring with simple, medium (edge stress equals centre stress),
and fixed support are shown in Figure 9.

Since, for plates supported on two opposite sides, the
stresses are linearly proportional to load q, there results s = n
= 16 and evaluation of B becomes a relatively simple matter.
Values of B for simple, fixed, and intermediate support (centre
stress equals edge stress) were calculated and found to be
respectively: 1.04×10^{-3}, 1.31×10^{-8}, 1.02×10^{-8}.

A reasonable design failure probability might be 0.001, i.e. 1 in 1000. Inserting this value of P_A, the several values of B, two values of A, a uniform pressure load of 0.20 psi and two duration times of 60 seconds and 1×10^8 seconds into equation (30) gives the results of Table V. These particular values of q and time can be considered to correspond only approximately to wind loading on a window and perhaps to snow loading on a skylight or to an aquarium window.

Because the examples are arbitrary, it is of more importance in Table V to discuss comparative, rather than actual thicknesses. In extending load duration from 60 seconds to 10^8 seconds, the thickness requirement is approximately doubled (2.3 times for support on all edges and 1.6 for two edge support. Changing plate area from 4 sq ft to 100 sq ft increases the ratio h/a by 54% for 4-edge support, but by only 26% for two-edge support. Decreasing the temperature from 21°C (68°F) to 0°C (32°F) decreases the thickness by 14% for 4-edge support and by 7% for 2-edge support. Two other interesting features arise: (1) for 2-edge support, the required plate thickness becomes approximately constant provided the edge stress is greater than that at the centre; and (2) since the time and area effect are different for 2- and 4-edge support, it is possible to have situations where the thickness requirements are the same in both cases.

DISCUSSION

The correlation of Figure 7 for soda-lime plate glass indicates the practicability of describing glass strength by equations (10) and (13). It appears likely that similar results can be obtained for glass of different compositions for which n and γ_0 presumably differ from those used herein for soda-lime glass.

A number of further comments are in order concerning strength and design:

(1) For correlations of the type of Figure 7, it is worth recalling that statistical populations may be chosen at will, for example, glass from all or from individual manufacture sources. It should also be emphasized that laboratory investigations on limited numbers of small samples will not yield strength results which are applicable to large plates of practical size which may be 100 times or more larger than the laboratory samples.

(2) Equation (10) does not consider very long-time delayed failure for which limiting stresses would be expected. Consequently, design on the basis of equation (10) will ordinarily prove somewhat conservative.

(3) It is important to avoid over-refinements to any single aspect of glass strength. Thus, for example, even though existing experimental data is limited, it would not appear reasonable to undertake further extensive and costly

experimental programs while little information is available on loads and climate (including the possibility of surface weathering damage and the mundane effects of dirt accumulation and periodic cleaning). In addition, residual stresses (tension and compression) of several hundred psi are usually present in large glass areas as a result of non-uniform heating and cooling during manufacture. On the other hand, as indicated by Table V, surface stress variations for real situations deserve further attention (most stress-analysis work of the past has tended to concentrate on maximum stresses, ignoring cumulative probability effects). Possibly, the simplest method to obtain these surface stresses will prove to be experimental (e.g. by direct measurement with strain gauges, in the manner of Kaiser). Since electronic computation will be involved in converting the results to failure probabilities, however, it may prove feasible to obtain entirely theoretical solutions from elastic theory. For plates in particular, the procedures developed by Levy (19) bear consideration: although complex they appear to offer great generality for large deflections with any type of edge support: meanwhile, equations (29) and (30) should prove of conceptual value in design.

REFERENCES

(1) Griffith, A.A. The Phenomena of rupture and flow in solids. Phil. Trans., Royal Society of London, Series A, Vol. 221; 1921, p. 163-198.

Griffith, A.A. The Theory of Rupture. Proceedings of the First International Congress of Applied Mechanics. Delft, 1924.

(2) Wiederhorn, S.M. Effects of environment on the fracture of glass. Conference on environment sensitive mechanical behaviour of materials. Baltimore, Maryland, June 1965, p. 293-316.

(3) Charles, R.J. Static Fatigue of Glass. J. Applied Physics, Vol. 29, No. 11, November 1958, p. 1549-1560.

(4) Charles, R.J. Dynamic fatigue of glass. J. Applied Physics, Vol. 29, No. 12, December 1958, p. 1657-1662.

(5) Charles, R.J. and W.B. Hillig. The kinetics of glass failure by stress corrosion. Symposium sur la résistance méchanique du verre et les moyens de l'améliorer. Florence, Italy. September 25-29, 1961, p. 511-527.

(6) Hillig, W.B. and R.J. Charles. Surfaces, stress-dependent surface reactions, and strength. High strength materials, Chapter 17, Edit. V.F. Zachay. John Wiley & Sons, N.Y. 1965.

(7) Marsh, D.M. Plastic flow and fracture of glass. Proc. Royal Society. Series A, Vol. 282, No. 1388, October 20, 1964, p. 33-43.

(8) Inglis, C.E. Stresses in a plate due to the presence of cracks and sharp corners. Trans. Institution of Naval Architects, Vol. 55, 1913, p. 219-241.

(9) Wiederhorn, S.M. Influence of water vapour on crack propagation in soda-lime glass. Journal of the American Ceramic Society, Vol. 50, No. 8, August 1967, p. 407-414.

(10) Mould, R.E. and R.D. Southwick. Strength and static fatigue of abraded glass under controlled ambient conditions. American Ceramic Society Journal, Vol. 42, No. 11, p. 542-547; Vol. 42, No. 12, p. 582-592.

- 2 -

(11) Kropschott, R.H. and Mikesell, J. Journal of Applied
Physics, 28, 1957, p. 610.

(12) Weibull, W. A statistical theory of the strength of
materials. Ingeniörsvetenskapsakademiens Handlingar
NR 151, Stockholm 1939, p. 1-45.

(13) Bowles, R. and B. Sugarman. The strength and deflection
characteristics of large rectangular glass panels under
uniform pressure. Glass Technology, Vol. 3, No. 5,
October 1962, p. 156-170.

(14) Libbey-Owens-Ford Glass Co., Toledo, Ohio, U.S.A. Glass
for Construction/1967 AIA - File No. 26-A-1967.

(15) Orr, L. Engineering properties of glass.in: Windows and
Glass in the exterior of buildings. Publication No. 478,
The Building Research Institute, Washington, 1957, p. 51-62.

(16) Mansfield, E.H. The bending and stretching of plates.
Pergamon Press, MacMillan Co., New York, 1964.

(17) Brown, W.G. Effect of Poisson's ratio for large deflec-
tions of elastic plates. (unpublished manuscript)

(18) Kaiser, R. Rechnerische u. experimentelle Ermittlung der
Durchbiegungen u. Spannungen v. quadratischen Platten bei
freier Auflagerung a. d. Rändern, gleichmässig verteilter
Last u. grossen Ausbiegungen. Zeitschrift für angewandte
Mathematik u. Mechanik. Band 16, Heft 2, April 1936,
s. 73-98.

(19) Levy, S. Bending of rectangular plates with large deflec-
tions. National Advisory Committee for Aeronautics,
Report No. 737, 1942, p. 1-19.

Appendix I - <u>One-dimensional stress equivalent of a two-dimensional stress</u>

For principal stresses σ_u, σ_v, the normal stress at angle χ to σ_u is:

$$\sigma_{nor} = \sigma_u \left(\cos^2\chi + \frac{\sigma_v}{\sigma_u} \sin^2\chi\right) \tag{A-1}$$

and, from equation (12)

$$\sigma_{\varepsilon_{nor}} = C\left\{\int_o^t \left(\frac{\sigma_{nor}}{T}\right)^n \cdot RH \cdot e^{-\gamma_o/RT} dt\right\}^{\frac{1}{n+1}} \tag{A-2}$$

Following Weibull (12), p. 14, $\sigma_{\varepsilon_{nor}}$ contributes partially to failure probability: the integrated probability is

$$P = 1 - \exp\left[-2k_1 C^m \int_{-\chi_o}^{+\chi_o} \left\{\left(\frac{\sigma_{nor}}{T}\right)^n \cdot RH \cdot e^{-\gamma_o/RT} dt\right\}^{\frac{m}{n+1}} d\chi \right. \tag{A-3}$$

Here, the integration limit χ_o is $\pi/2$ when both principal stresses are tensile, otherwise:

$$\chi_o = \tan^{-1}\sqrt{-\frac{\sigma_u}{\sigma_v}} \tag{A-4}$$

Now, for a one-dimensional stress σ_{u_1}, i.e. $\sigma_{v_1} = o$,

$$P = 1 - \exp\left[-2k_1 C^m \left\{\int_o^t \left(\frac{\sigma_{u_1}}{T}\right)^n \cdot RH \cdot e^{-\gamma_o/RT} dt\right\}^{\frac{m}{n+1}} \int_{-\chi_o}^{+\chi_o} (\cos^2\chi)^{\frac{mn}{n+1}} d\chi\right] \tag{A-5}$$

Also,

$$\int_{-\chi_0}^{+\chi_0} (\cos^2\chi)^{\frac{mn}{n+1}} \, d\chi = \sqrt{\pi} \; \frac{\Gamma(\frac{2m_1+1}{2})}{\Gamma(m_1+1)} \tag{A-6}$$

where $\quad m_1 = \dfrac{mn}{n+1}$

Setting: $\quad C\{\int_o^t (\frac{\sigma_{u_1}}{T})^n \cdot RH \cdot e^{-\gamma_0/RT} dt\}^{\frac{1}{n+1}} = \sigma_\epsilon \tag{A-7}$

and equating (A-3) and (A-5) gives:

$$\sigma_\epsilon = C[\frac{1}{\sqrt{\pi}} \cdot \frac{\Gamma(m_1+1)}{\Gamma(\frac{2m_1+1}{2})} \int_{-\chi_0}^{+\chi_0} \{\int_o^t (\frac{\sigma_u}{T})^n (\cos^2\chi + \frac{\sigma_v}{\sigma_u} \sin^2\chi)^n \cdot RH \cdot e^{-\gamma_0/RT} dt\}^{\frac{m}{n+1}} d\chi]^{\frac{1}{m}} \tag{A-8}$$

This is the one dimensional stress-equivalent of a two-dimensional stress for the conditions of equations (10) and (12).

Appendix II - Approximations

In general, the surface stresses for most plates will not vary linearly with applied load, thus σ_v/σ_u will be time dependent. To avoid the computation difficulties which this introduces into evaluation of equation (A-8), quasi-linearity will be assumed. Thus, with

$$C\{\int_o^t (\frac{\sigma_u}{T})^n \cdot RH \cdot e^{-\gamma o/RT}dt\}^{\frac{1}{n+1}} = \sigma_{u\epsilon} \tag{A-9}$$

equation (A-8) becomes:

$$\sigma_\epsilon = \sigma_{u\epsilon}[\frac{1}{\sqrt{\pi}} \cdot \frac{\Gamma(m_1+1)}{\Gamma(\frac{2m_1+1}{2})} \int_{-\chi_o}^{+\chi_o} (\cos^2\chi + \frac{\sigma_v}{\sigma_u} \sin^2\chi)^{m_1} d\chi]^{\frac{1}{m}} \tag{A-10}$$

$$\text{and;} \quad (\frac{\sigma_\epsilon}{\sigma_{\epsilon c}})^m = \frac{\sigma_u^{m_1} \int_{-\chi_o}^{+\chi_o} (\cos^2\chi + \frac{\sigma_v}{\sigma_u} \sin^2\chi)^{m_1} d\chi}{\sigma_{uc}^{m_1} \int_{-\chi_o}^{+\chi_o} (\cos^2\chi + \frac{\sigma_{vc}}{\sigma_{uc}} \sin^2\chi)^{m_1} d\chi} \tag{A-11}$$

$$= [f(\frac{x}{a}, \frac{y}{\ell})]^m$$

Here, subscript c signifies a reference location.

The large exponent n = 16 indicates weak time-dependence. Thus, instantaneous stress values could be inserted into equation (A-11) for determination of I by equation (16). The procedure can be improved, however, as follows:

In equation (15) set;

$$\eta = I \; \sigma_{\epsilon c}^{m} \tag{A-13}$$

thus, by virtue of equations (9) and (A-10)

$$\sigma_{\epsilon c}^{m} = \eta/I = C^{m} \cdot r[\int_{o}^{t} (\frac{\sigma_{uc}}{T})^{n} \cdot RH \cdot e^{-\gamma_{o}/RT} \; dt]^{\frac{m}{n+1}} \tag{A-14}$$

where $r = [\frac{1}{\sqrt{\pi}} \frac{\Gamma(m_{1}+1)}{\Gamma(\frac{2m_{1}+1}{2})} \int_{-\chi_{o}}^{+\chi_{o}} (\cos^{2}\chi + \frac{\sigma_{vc}}{\sigma_{uc}} \sin^{2}\chi)^{m_{1}} \; d\chi] \cdot$ (A-15)

Now, re-insert I and r under the integral sign in (A-14), i.e.:

$$\eta = C^{m}\{\int_{o}^{t} (rI)^{\frac{n+1}{m}} \cdot (\frac{\sigma_{uc}}{T})^{n} \cdot RH \cdot e^{-\gamma_{o}/RT} \; dt\}^{\frac{m}{n+1}} \tag{A-16}$$

Appendix III - Table VI (Weibull, p. 13 - Table I)

Parameter $M = \dfrac{m(s+b)}{n+1}$	$j = \int_0^\infty e^{-z^m} dz$	Coefficient of Variation
1	1.000	1.00
2	0.886	0.52
3	0.896	0.36
4	0.908	0.28
8	0.940	0.16
16	0.965	0.09
∞	1.000	0.00

Appendix IV - Determination of Parameter k

Using Weibull's development (12) page 13, it can readily be shown that:

$$\frac{1}{k} = \frac{1}{i}\left\{\frac{RH}{T^n}\cdot e^{-\gamma_0/RT}\right\}^{\frac{m}{n+1}}\cdot C^m\left\{B\ E^{n-s}\right\}^{\frac{m}{n+1}}\left\{\frac{A}{A_o}^{\frac{n+1}{m}}\left(\frac{a}{h}\right)^{4s-2n}\cdot\frac{b\bar{t}}{s+b}\cdot\bar{q}^s\right\}^{\frac{m}{n+1}} \qquad (A-17)$$

Here: $\quad i = \left\{\int_o^\infty \exp\left[-z^{\frac{m(s+b)}{n+1}}\right]dz\right\}^{\frac{m(s+b)}{n+1}} = 0.651,$

where the integrated value is obtained from Table VI for $\frac{m(s+b)}{n+1} = 5.5.$

A value of 9.33×10^{18} for the last bracketted term raised to its exponent 7.3/17 in equation (A-17) is determined directly from Figure 7.

Because Kaiser measured the two-dimensional stress distribution over the plate surface, it is possible to obtain an independent value of rI (equation (17)) or of $(rI)^{\frac{n+1}{m}}\sigma_c^n$ for insertion into equation (19) to obtain B: this is the last remaining unknown in equation (A-17).

Kaiser measured both bending and membrane stresses at 49 locations on a steel plate surface. Mean values were then determined giving the stresses at 10 locations on a one-eighth (i.e. symmetrical) segment of the plate.

For present purposes, the stresses were first converted by the method (17) to account for the difference in Poisson's ratio for glass and steel. With a value of $m_1 = 6.9$, equation (A-11) was then calculated for all locations. The integration indicated in equation (16) was then performed to obtain a value of I. In the case of a square plate, the factor r (equation (A-15)) is a permanent constant since $\sigma_{uc} = \sigma_{vc}$. The product $r I \sigma_{uc}^{6.9} = \{(rI)^{\frac{n+1}{m}} \sigma_{uc}^{n}\}^{\frac{m}{n+1}}$ was then computed and plotted against the corresponding value of $\frac{q}{E}(\frac{a}{h})^4$ in Figure 8. All computations were carried out electronically with occasional rough checks by hand.

In the form of equation (19), Figure 8 yields $B = 3.02 \times 10^{-6}$ for the extreme right of the figure; this is the range corresponding to bowles and Sugarman's tests on 1/4" and 3/8" plates. (Note: the corresponding slope in Figure 8 gives $\frac{sm}{n+1} = 4.8$, in moderately good agreement with the earlier determined value of 5.3.)

Reference conditions:

Room temperature (295°K) and 50% relative humidity are suitable reference environment conditions.

An easily remembered standard loading rate of $\beta_o = 100$ psi per second is suitable.

With these two conditions, the factor $\{\frac{RH}{T^n} \cdot e^{-\gamma_o/RT}\}^{\frac{m}{n+1}} \cdot C^m$ in equation (A-17) becomes $\{\beta_o(n+1)\}^{\frac{m}{n+1}} = 1700^{\frac{m}{n+1}}$, from equation (10). Inserting the various constants, and with $E = 10^7$ psi, equation (A-17) yields:

$$k = 5 \times 10^{-30} \text{ psi}^{-7.3}$$

TABLE II--TEST DATA BY BOWLES AND SUGARMAN (13) FOR 41" x 41" GLASS PLATES*, UNIFORMLY LOADED

	Nominal Thickness	Mean Thickness (inches)	No. of Samples	Mean Bursting Pressure (psi)	Coefficient of Variation (%) (1)	Mean Center Deflection (inches)	Coefficient of Variation (%) (2)	Average Time to Failure (secs)	b_1 (equation 28)	b_2 (2) ÷ (1)	$\frac{\nu_q}{\nu_w} (\frac{}{b_1})$
plate glass	(1/8 in.	0.122	40	0.754	17.3	0.760	8.6	35.1	0.42	0.50	21
	3/16 in.	0.197	30	1.412	18.0	0.726	9.2	34.1	0.44	0.50	21
	1/4 in.	0.245	30	1.811	25.0	0.651	12.1	30.9	0.49	0.47	25
	3/8 in.	0.373	30	3.625	23.7	0.610	14.0	29.4	0.63	0.58	22
sheet glass	(24 oz.	0.110	30	0.692	14.0	0.807	7.6	37.0	0.45	0.56	17
	32 oz.	0.158	30	1.369	15.9	0.870	7.2	38.1	0.42	0.45	17
	(3/16 in.	0.195	30	1.910	20.5	0.860	11.0	37.6	0.42	0.52	26

* Plates were tested in a 40" x 40" opening on a rubber gasket.
  Thus, the effective plate size is close to 40.5" x 40.5".

TABLE III – SELECTED SQUARE PLATES TESTED
IN DEVELOPMENT OF FIGURE (4)

	Plate Size	Area (sq. ft.)	$\bar{q}$(Fig. 4)	$\frac{\bar{q}}{E}(\frac{a}{h})^4$	$(\frac{W_o}{h})$ (equn. 24)	W_o (inches)	$\bar{t}$ (sec)	b (equn. 26)	$b\bar{t}(\frac{b\bar{t}}{s+b})^{\frac{1}{s}}$
(1)	8' x 8' x 3/4"	64	1.85	51	1.65	1.24	930	0.62	580 1.36
(2)	6' x 6' x 1/2"	36	1.70	74	2.05	1.02	770	0.55	420 1.33
(3)	8.94' x 8.94' x 1/2"	80	0.77	165	3.05	1.52	1140	0.47	540 1.36
(4)	10' x 10' x 1/2"	100	0.62	205	3.40	1.70	1270	0.45	570 1.36
(5)	6' x 6' x 3/8"	36	1.17	160	3.00	1.12	840	0.47	390 1.32
(6)	8' x 8' x 3/8"	64	0.66	285	3.85	1.44	1080	0.44	470 1.34
(7)	10' x 10' x 3/8"	100	0.42	445	4.75	1.78	1340	0.42	560 1.36

TABLE IV - EFFECT OF LOAD DURATION AND PLATE AREA

Plate Size (L-O-F tests)	(1) Mean Bursting Pressure psi $\bar{q}$	(2) h_e † (inches)	(3) Indicated Bursting Pressure Fig.(6) $\bar{\bar{q}}$	(4) Ratio $\bar{\bar{q}}/\bar{q}$	(5) Load* Duration Effect	(6) Area** Effect	(7) (5)x(6)
1) 8' x 8' x 3/4"	1.85	0.32	2.9	1.5	1.34	1.38	1.8
2) 6' x 6' x 1/2"	1.70	0.28	2.4	1.4	1.31	1.24	1.6
3) 8.94' x 8.94' x 1/2"	0.77	0.19	1.4	1.8	1.34	1.44	1.9
4) 10' x 10' x 1/2"	0.62	0.17	1.2	1.9	1.34	1.51	2.0
5) 6' x 6' x 3/8"	1.17	0.21	1.6	1.4	1.30	1.24	1.6
6) 8' x 8' x 3/8"	0.66	0.16	1.1	1.7	1.33	1.38	1.8
7) 10' x 10' x 3/8"	0.42	0.13	0.82	1.9	1.34	1.51	2.0

* Defined as: $\left\{ \left[\frac{b\bar{t}}{12.3+b}\right]_{LOF} \middle/ \left[\frac{b\bar{t}}{12.3+b}\right]_{BS} \right\}^{\frac{1}{12.3}}$

** Defined as: $\{A_{LOF} / A_{BS}\}^{\frac{1}{5.3}}$

† $h_e = \frac{a}{40.5} \times h$, i.e. h_e is the equivalent thickness for the Bowles-Sugarman tests. (a is the plate width in inches)

TABLE V - PLATE GLASS THICKNESSES TO WITHSTAND
A CONSTANT UNIFORM PRESSURE LOAD OF 0.2 psi
WITH FAILURE PROBABILITY OF 1 IN 1000

| Type of Support	2' x 2' plate						10' x 10' plate					
	60 sec Duration at 21°C		10^8 sec Duration at 21°C		10^8 sec Duration at 0°C		60 sec Duration at 21°C		10^8 sec Duration at 21°C		10^8 sec Duration at 0°C	
	h/a $\times 10^3$	h (in.)	h/a $\times 10^3$	h (in.)	h/a $\times 10^3$	h (in.)	h/a $\times 10^3$	h (in.)	h/a $\times 10^3$	h (in.)	h/a $\times 10^3$	h (in.)
Simple (all edges)	3.2	0.08	7.3	0.18	6.3	0.15	4.9	0.59	11.1	1.34	9.7	1.15
Simple (2 opposite edges)	7.3	.18	11.5	.28	10.7	0.25	9.3	1.11	14.6	1.74	13.5	1.60
Medium (2 opposite edges)	5.2	.12	8.2	.21	7.6	0.18	6.5	.78	10.2	1.22	9.4	1.13
Fixed (2 opposite edges)	5.2	.12	8.2	.21	7.6	0.18	6.4	.78	10.1	1.22	9.4	1.13
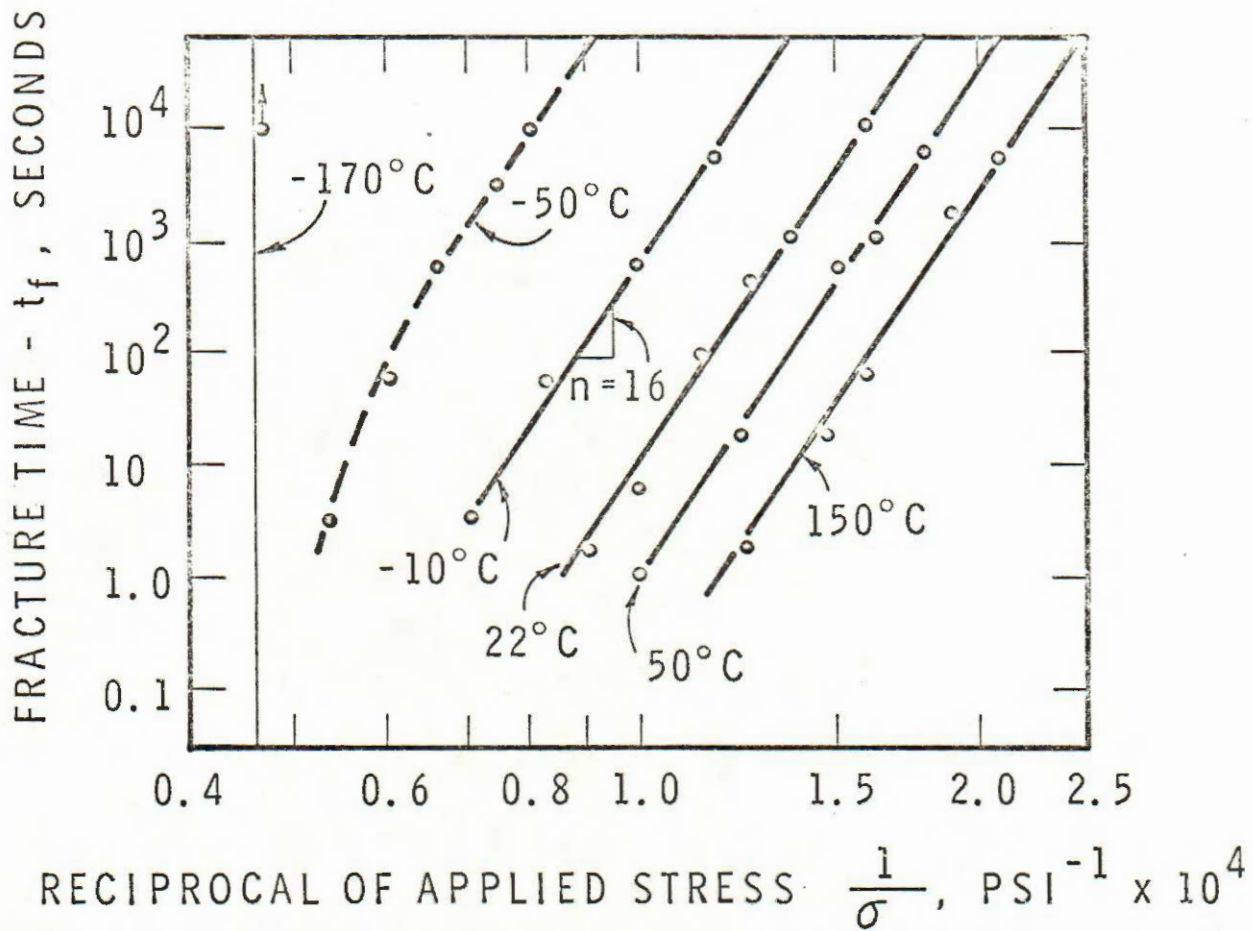
FIGURE 1

EXPERIMENTAL RESULTS FROM STATIC
FATIGUE TESTING OF SODA LIME GLASS
RODS (CORNING 0080) IN SATURATED
WATER VAPOR.   AFTER CHARLES (3)

BR 4276-2

The graph displays a straight line plotted with data points. The y-axis is labeled "AVERAGE FAILURE STRESS, PSI" ranging from 10,000 to 16,000. The x-axis is labeled "LOADING RATE, INCHES/MINUTE" with values 0.005, 0.05, and 0.5. Annotated on the graph:

$$\text{Slope} = \frac{1}{n+1} \approx \frac{1}{18}$$
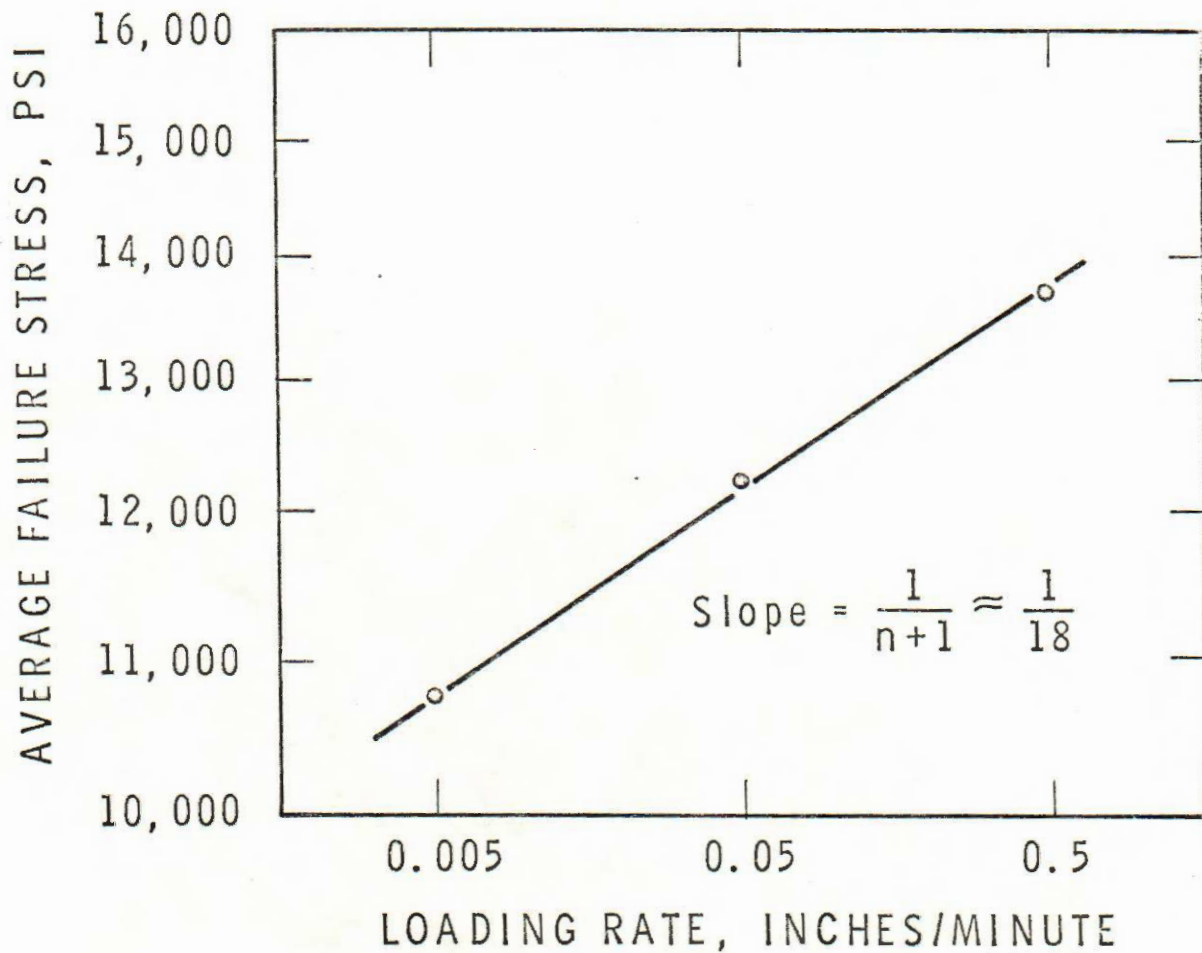
FIGURE 2

EFFECT OF CONSTANT LOADING RATE ON AVERAGE
FAILURE STRESS AT 25°C (After Charles (4))

BR 4276 - 12
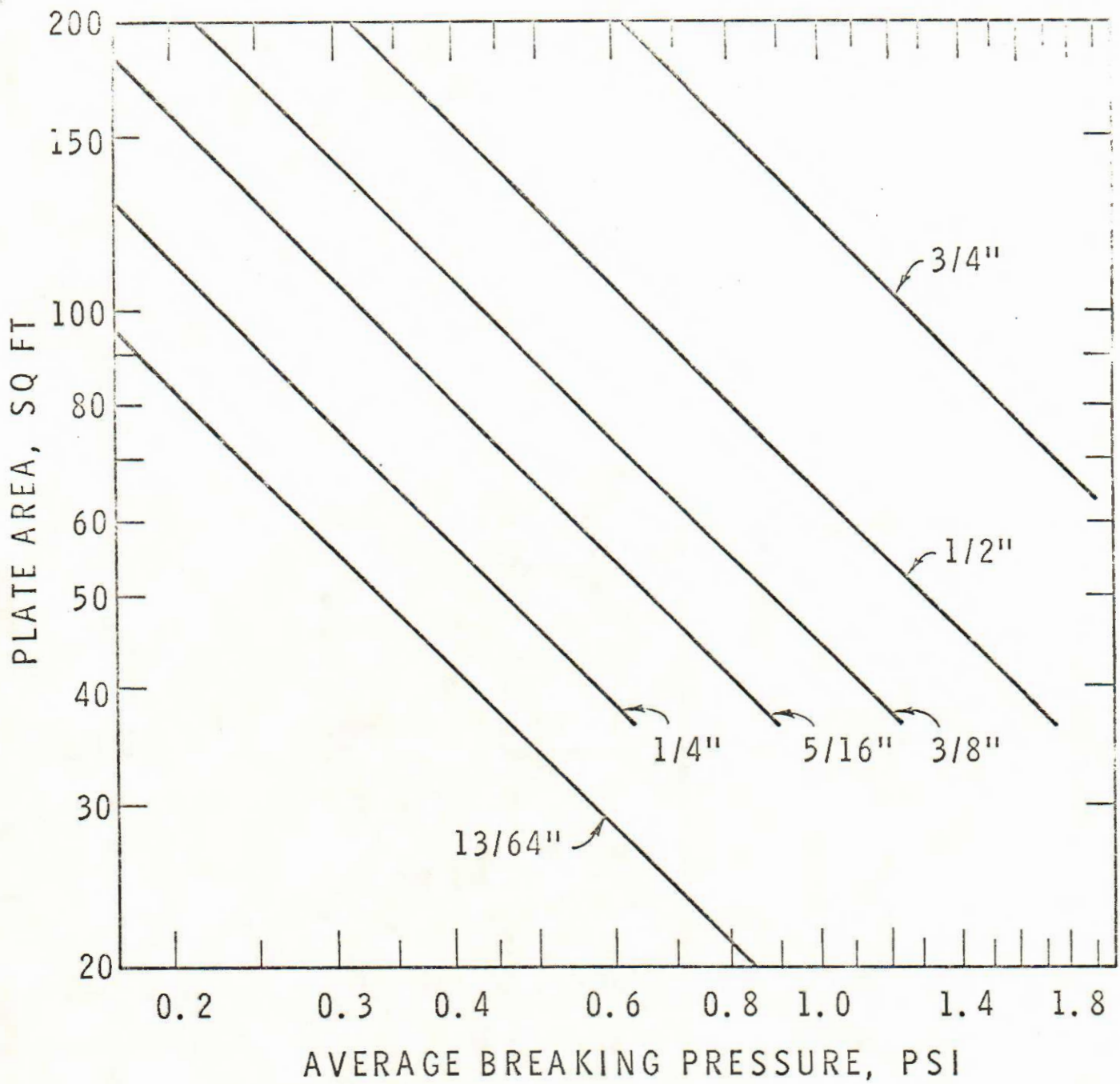
FIGURE 4

STRENGTH CHART (LIBBEY - OWENS - FORD GLASS CO. (14))
(Note: Manufacture Tolerances as Indicated in (14) Have
        Been Re-applied)

BE 4276-4

FRACTURE TIME AT $\sigma = 10,000 \times \left(\dfrac{296}{T}\right)$, PSI (from Fig. 1),

$\alpha = 1$,
$\gamma_0 = 25$
KCAL/MOL

$\dfrac{\gamma_0}{2.3R}$

$-50^\circ C$

$\dfrac{\gamma_0}{2.3R}$

$\alpha = 0$,
$\gamma_0 = 18.8$
KCAL/MOL

$-10^\circ C$

$22^\circ C$

$50^\circ C$
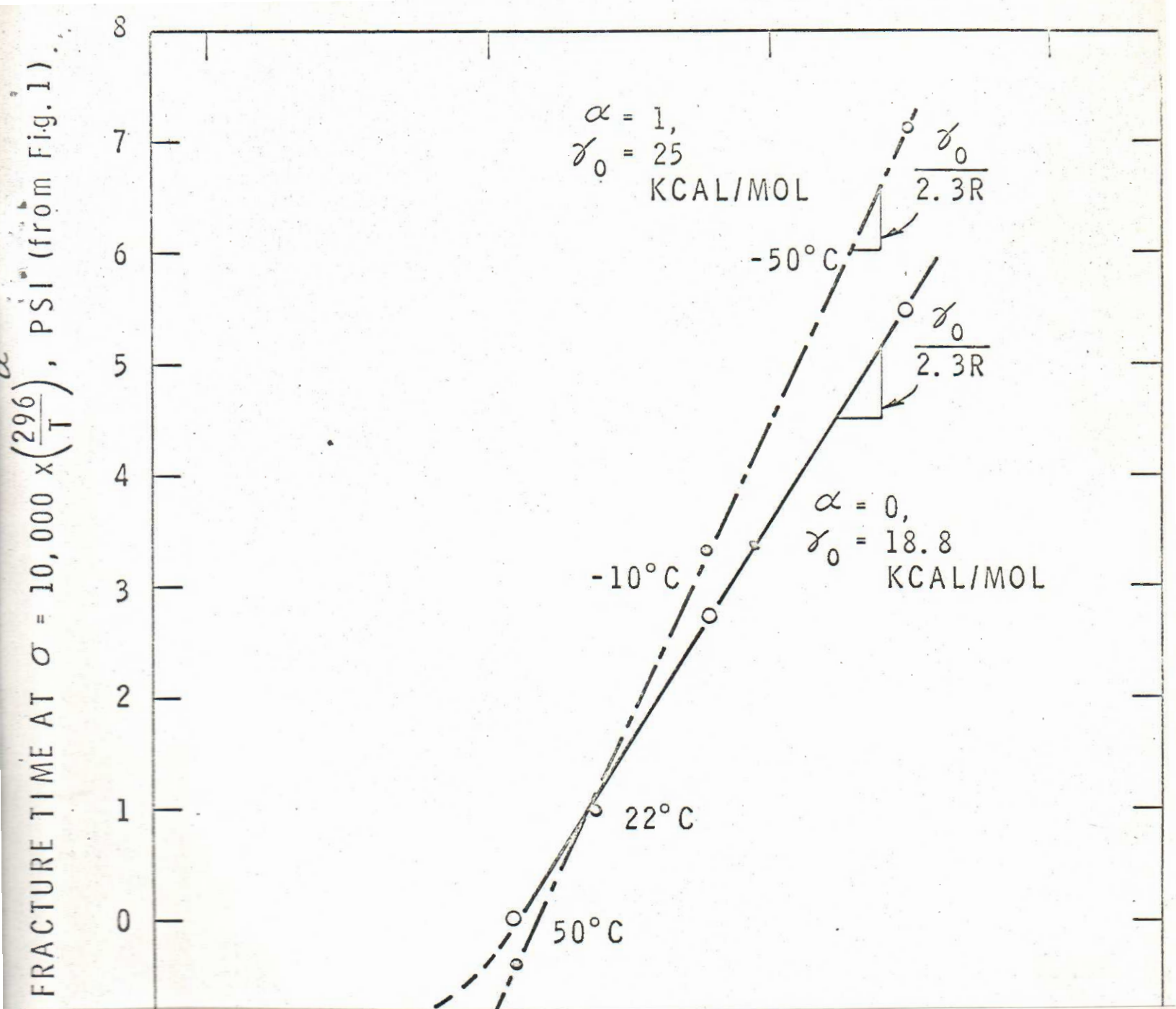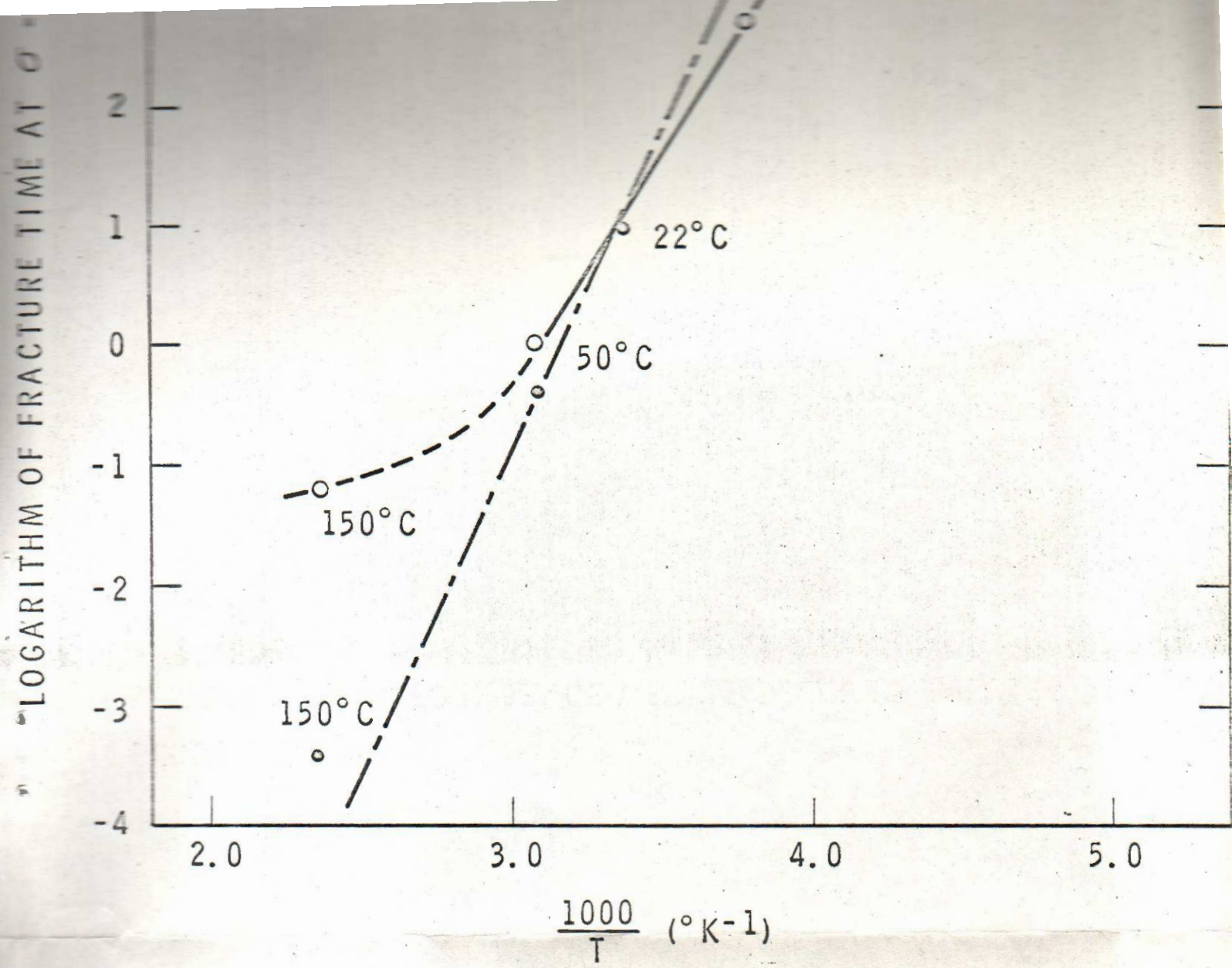
FIGURE 3

TEMPERATURE DEPENDENCE OF THE DELAYED FAILURE PROCESS

BR 4276 -13

LEGEND

- ○ Bowles - Sugarman (Plate)
- ○ Bowles - Sugarman (Sheet)
- □ Orr   (Plate)
- ▣ Kaiser (Steel, Converted)

$\frac{q}{E}\left(\frac{a}{h}\right)^4$

w_0/h
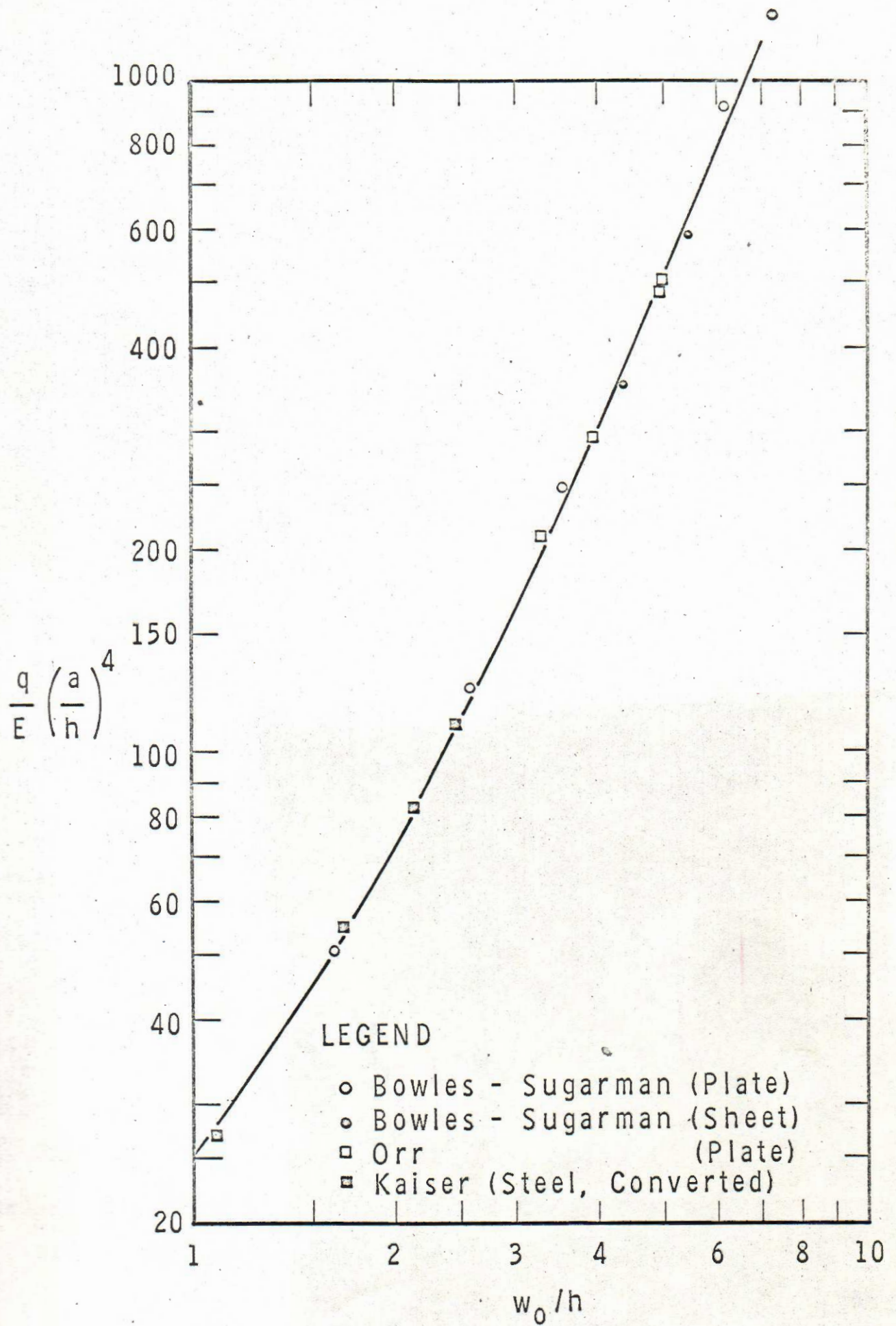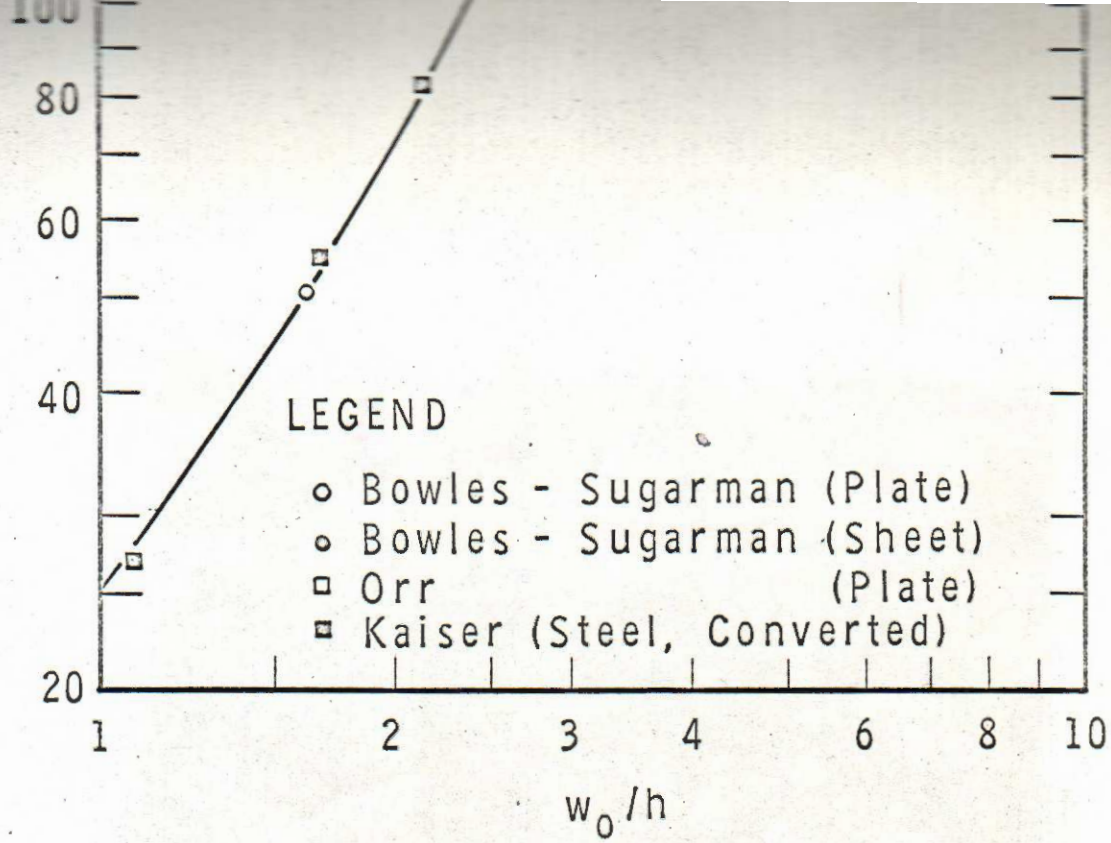
FIGURE 5

LOAD DEFLECTION RELATIONSHIP FOR UNIFORMLY LOADED, SQUARE GLASS PLATES WITH SIMPLE SUPPORT

BR 1276-7
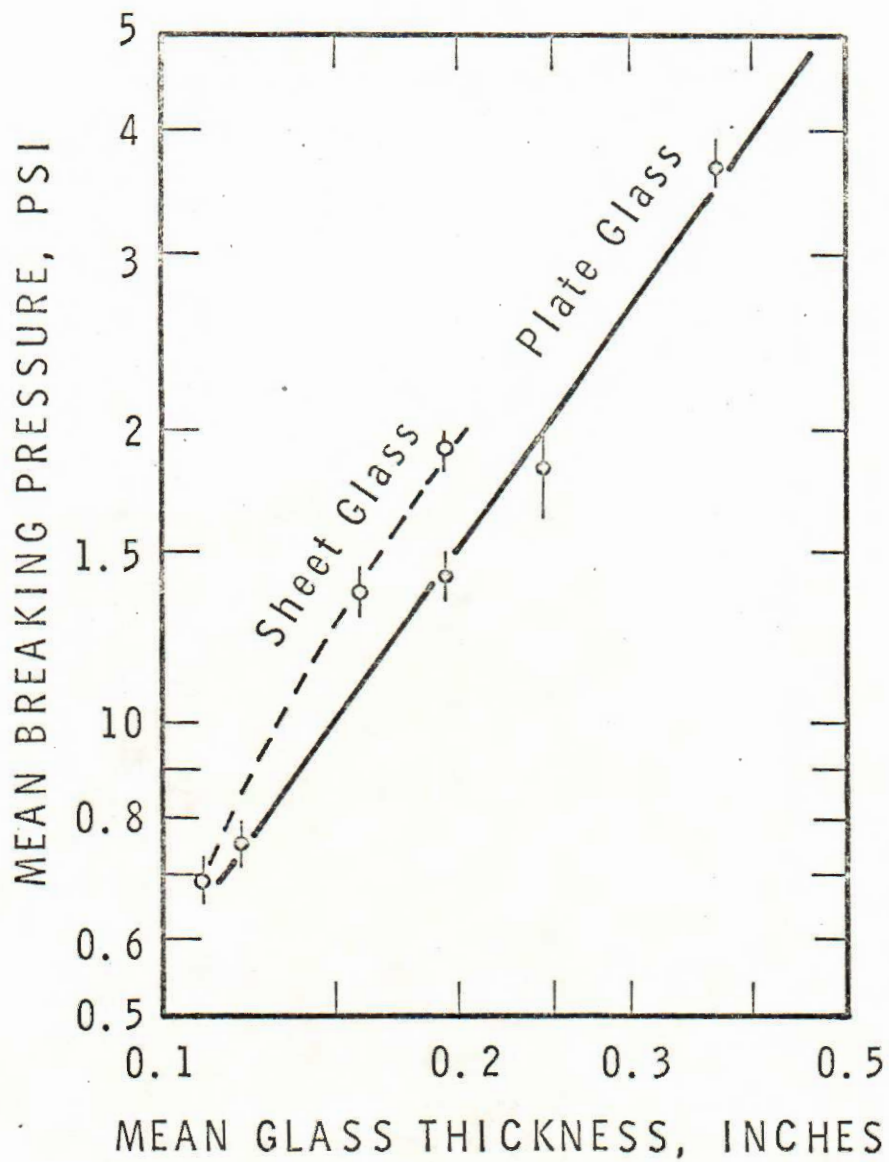
FIGURE 6

MEAN BREAKING PRESSURE AS DEPENDENT
ON PLATE THICKNESS. SIMPLY-SUPPORTED
SQUARE PLATES, (BOWLES & SUGARMAN)

BG 4276 - B
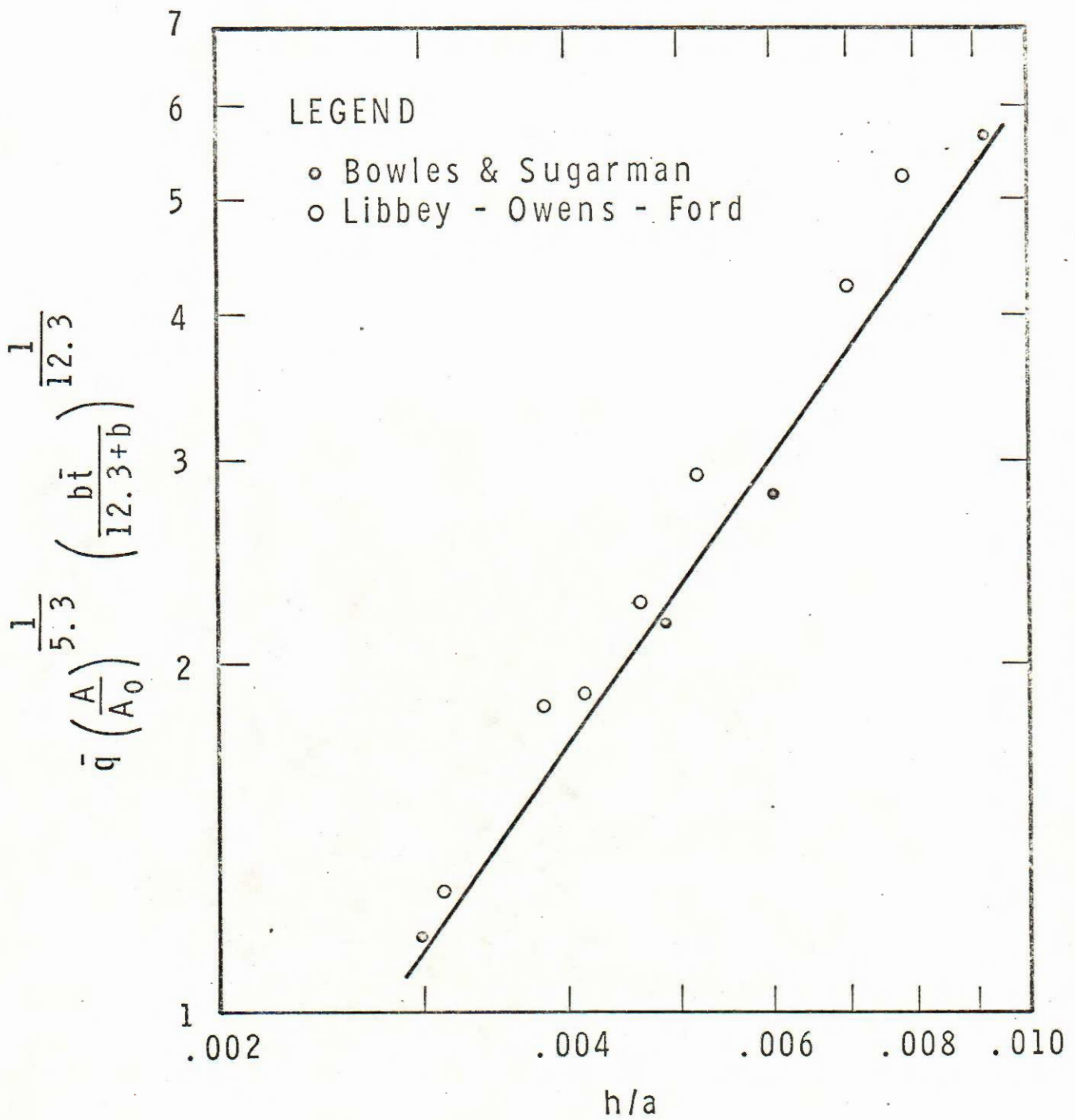
FIGURE 7

CORRELATION OF STRENGTH OF UNIFORMLY
LOADED SQUARE GLASS PLATES FROM TWO
INDEPENDENT SOURCES (SODA-LIME PLATE
GLASS)

BR 4276 - 9
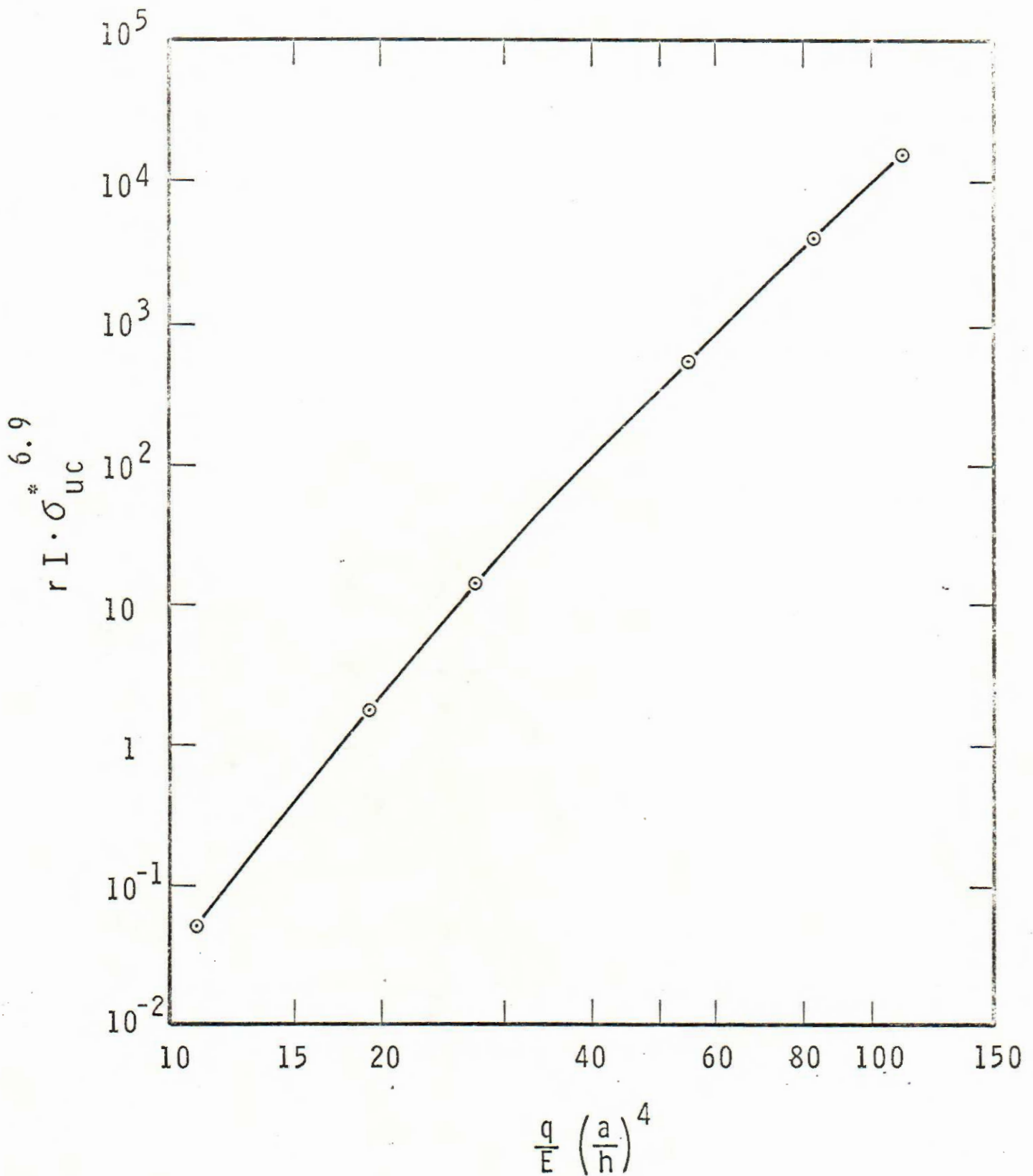
FIGURE 8

PROBABILITY PARAMETERS DERIVED FROM STRESS
DISTRIBUTION DATA OF KAISER (18). SIMPLY
SUPPORTED SQUARE GLASS PLATE.

FIGURE 9

TENSILE STRESS DISTRIBUTION IN
RECTANGULAR PLATES SUPPORTED
ON TWO OPPOSITE SIDES.
(CORRESPONDS TO LONG NARROW
PLATES)

BR 4276-11